

## Control of material transport and reaction mechanisms by metastable mineral assemblages: An example involving kyanite, sillimanite, muscovite and quartz

C. T. FOSTER, JR.

Geology Department, University of Iowa, Iowa City, Iowa 52242, U.S.A.

**Abstract**—Metastable mineral assemblages strongly influence reaction mechanisms and material transport when a new mineral grows in a metamorphic rock. The effects exerted by the metastable assemblages on the reactions that take place when sillimanite grows in a kyanite-bearing rock are examined using metastable elements of activity diagrams and irreversible thermodynamic principles. The results show that a commonly inferred reaction mechanism, where muscovite assists in the growth of sillimanite at the expense of kyanite, is a consequence of material transport constraints imposed by a metastable mineral assemblage in the matrix that separates growing sillimanite from dissolving kyanite.

### INTRODUCTION

ONE OF THE PRIMARY controls on mineral textures that develop during metamorphism is the distribution of minerals in a rock at the time when a new mineral nucleates. The distribution of the new mineral is strongly influenced by the abundance and location of other minerals with favorable nucleation sites for it. Once the new mineral has nucleated and begun to grow, the material transport and reaction mechanisms that develop are controlled by local equilibrium with metastable mineral assemblages along the transport path.

For example, consider the reaction mechanisms that develop in a rock containing the phases kyanite + muscovite + quartz + water when the temperature changes along the isobaric heating path shown on the *P-T* diagram in Fig. 1a. This path crosses the sillimanite isograd by passing from the kyanite stability field into the sillimanite stability field. At temperatures in the kyanite field, before the sillimanite isograd is crossed (point I, Fig. 1a), the stable mineral assemblage will be kyanite + muscovite + quartz + water. When the temperature rises to the point where the univariant curve representing equilibrium between kyanite and sillimanite is reached (the theoretical sillimanite isograd: point II, Fig. 1a), sillimanite becomes stable with kyanite. However, no sillimanite forms at the theoretical isograd because the reaction kyanite → sillimanite must be overstepped by a finite amount to form sillimanite nuclei (FISHER, 1977; RIDLEY and THOMPSON, 1986). The absence of sillimanite nuclei allows the metastable kyanite-bearing assemblage to persist into the sillimanite stability field without reacting (point III, Fig. 1a). A schematic illustration of the textures present in the rock at the

pressures and temperatures represented by points I, II, and III (Fig. 1a) is shown in Fig. 1b.

Sillimanite nuclei first form in sites in the rock with the lowest activation energy for nucleation of sillimanite. Under many metamorphic conditions, the low energy sites for sillimanite nucleation in pelites appear to be in micas, because this is where sillimanite is commonly first observed with increasing metamorphic grade (CHINNER, 1961; CARMICHAEL, 1969; YARDLEY, 1989). Once sillimanite nuclei form in the rock, either of two things happen. If the nucleation rate is low, and only a few nuclei form before appreciable reaction takes place in the rock, reaction cycles develop that involve material transport between the few sites where sillimanite is growing and the sites where kyanite is dissolving (Fig. 1c). This type of reaction mechanism, which uses micas as catalysts in the reaction, was first recognized by CARMICHAEL (1969) and it probably indicates that the sillimanite forming reaction is never overstepped by a large amount (point IV, Fig. 1a). If the nucleation rate is high, and little or no reaction takes place until nuclei have formed in most sites in the rock, nuclei of sillimanite will be present in the immediate vicinity of kyanite. Then the reaction mechanism will involve direct replacement without much material transport or the use of mineral catalysts (Fig. 1d).

### REACTION MECHANISMS, MATERIAL TRANSPORT, AND METASTABLE ASSEMBLAGES

When sillimanite nucleates and begins to grow, many of the local mineral assemblages present in the rock are metastable with respect to the assemblage sillimanite + muscovite + quartz + water. These metastable assemblages exert a strong control

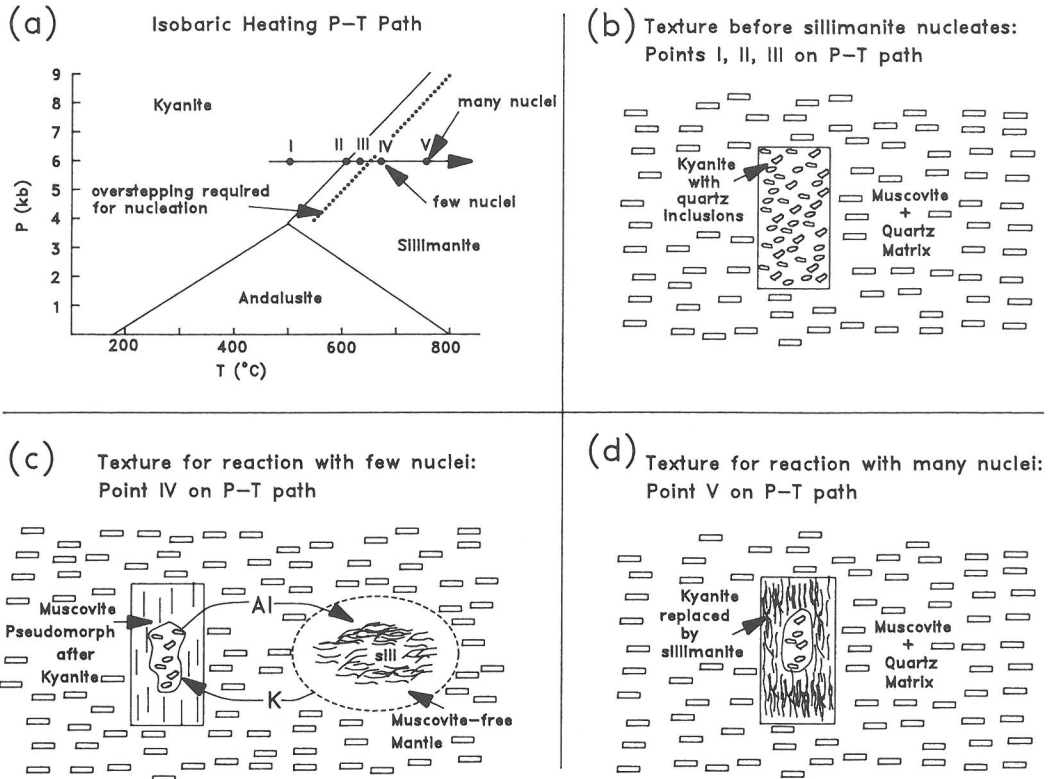


FIG. 1. (a) Pressure-temperature path followed by a kyanite-bearing rock that passes into the sillimanite field. Points I, II, III, IV, and V represent  $P$ ,  $T$  conditions along the path that are discussed in the text. The dotted line schematically illustrates that some overstepping is needed to form sillimanite nuclei. The exact amount of overstepping required to form sillimanite nuclei is presently unknown. (b) Sketch of the texture existing prior to the nucleation and growth of sillimanite (points I, II, and III on Fig. 1a). The large vertical rectangle represents a kyanite poikiloblast with quartz inclusions. The many small horizontal rectangles represent muscovite crystals surrounded by quartz. (c) Sketch of the texture that develops if reaction takes place when nuclei have only formed in the sites most favorable for nucleation (point IV on Fig. 1a). The vertical line pattern inside the large vertical rectangle represents a muscovite pseudomorph after kyanite. The irregular lines inside the ellipse represent fibrolitic sillimanite. The blank area within the ellipse is a muscovite-free quartz mantle that surrounds the fibrolite. Kyanite poikiloblast and matrix muscovite patterns are the same as in Fig. 1b. Arrows labelled Al and K represent material transport of aluminum and potassium between reaction sites. (d) Sketch of the texture that develops if reaction takes place when nuclei have formed at many sites in the rock (point V on Fig. 1a). The irregular lines inside the vertical rectangle represent fibrolitic sillimanite that has replaced kyanite. Matrix muscovite and kyanite poikiloblast patterns are the same as in Fig. 1b.

over the type of textures that develop during the conversion of kyanite to sillimanite, particularly when the reaction mechanisms involve material transport under local equilibrium conditions. The effects of the metastable assemblages can be illustrated by considering the activity diagrams shown in Fig. 2. These diagrams show the distribution of stable mineral phases as a function of the activity of potassium and aluminum when temperature changes from conditions where kyanite is stable to conditions where sillimanite is stable. The diagrams in Fig. 2 were constructed using Schreinemaker's

methods (ZEN, 1966; YARDLEY, 1989) and the thermodynamic data base of HELGESON *et al.* (1978). The reactions represented by univariant lines in these diagrams have been written to conserve silica, conforming to a silica-fixed reference frame (BRADY, 1975), which is equivalent to an inert marker reference frame in quartz-bearing rocks under a hydrostatic stress (FOSTER, 1981). This reference frame was chosen because many geologists intuitively think of material transport with respect to an inert marker reference-free frame. Water is not labeled as a phase on Fig. 2, but the diagrams are

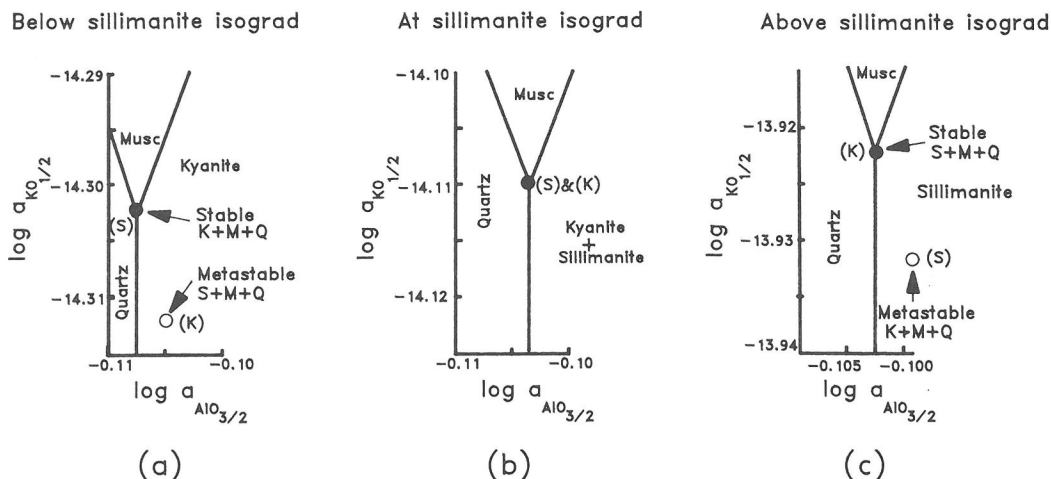


FIG. 2. Diagrams showing stable univariant lines, stable divariant fields, the sillimanite-absent (S) invariant point and the kyanite-absent (K) invariant point as a function of the activities of aluminum and potassium. S + M + Q stands for the co-existence of sillimanite + muscovite + quartz. K + M + Q stands for the co-existence of kyanite + muscovite + quartz. Water is assumed to be in equilibrium with all assemblages. See text for explanation of choice of components and standard states. Note that the tick marks on the axes have different values on each diagram. (a) Conditions 10°C below the sillimanite isograd: 607°C, 6 kb. The kyanite-absent invariant point is metastable. (b) Conditions at the theoretical sillimanite isograd: 617°C and 6 kb. The sillimanite-absent and kyanite-absent invariant points are coincident; both are stable. (c) Conditions 10°C above the sillimanite isograd: 627°C, 6 kb. The sillimanite-absent invariant point is metastable.

calculated for the situation where the solid phases were in equilibrium with pure water at the  $T$  and  $P$  of interest. The activities of potassium and aluminum have been expressed in terms of oxide components with the standard state chosen so that  $\text{KO}_{1/2}$  has unit activity when the system is saturated with respect to potassium oxide and  $\text{AlO}_{3/2}$  has unit activity when the system is saturated with respect to corundum. This convention has been chosen for convenience to avoid complications involving the uncertainties of speciation, particularly of aluminum, at metamorphic temperatures and pressures (WALTHER, 1986; WOODLAND and WALTHER, 1987; EUGSTER and BAUMGARTNER, 1987). If one wishes to specify a dominant species at the pressure and temperature of interest, the diagrams can be easily converted to aqueous species by calculating equilibrium constants for reactions such as  $\text{KO}_{1/2} + \text{HCl} \rightarrow \text{KCl} + 0.5 \text{H}_2\text{O}$  and  $\text{AlO}_{3/2} + 1.5 \text{H}_2\text{O} \rightarrow \text{Al}(\text{OH})_3$ . The activities can then be recast in terms of the new species.

At temperatures in the kyanite stability field (point I, Fig. 1a), local equilibrium will keep the activities of aluminum and potassium in the rock at the stable invariant point where the minerals kyanite + muscovite + quartz + water coexist. This invariant point is labelled (S) on Fig. 2a because it represents the conditions where the sillimanite-ab-

sent assemblage is in equilibrium. All sillimanite-bearing assemblages are metastable at temperatures and pressures where kyanite is stable. For example, on Fig. 2a, the activities where the assemblage sillimanite + muscovite + quartz + water is in equilibrium are given by the position of the kyanite-absent (K) invariant point. It is a metastable invariant point located in the kyanite stability field because sillimanite + muscovite + quartz + water is less stable than kyanite + water at 607°C and 6 kb. As the temperature rises and conditions in the rock approach the sillimanite stability field, the differences in chemical potentials between the kyanite-absent (K) invariant point and the sillimanite-absent (S) invariant point decrease. When the theoretical sillimanite isograd is reached (point II, Fig. 1a), the two invariant points (K) and (S) are coincident, indicating that both kyanite-bearing and sillimanite-bearing assemblages are stable (Fig. 2b). However, no sillimanite forms at this time because the reaction has not been overstepped and no sillimanite nuclei are present in the rock. As the temperature continues to rise, sillimanite becomes more stable than kyanite (point III, Fig. 1a); the sillimanite-absent (S) invariant point becomes metastable while the kyanite-absent (K) invariant point becomes stable (Fig. 2c).

If sillimanite has not nucleated in the rock, the

activities of potassium and aluminum are constrained to lie at the metastable sillimanite-absent invariant point (S) on Fig. 2c because the most stable assemblage present in the rock is kyanite + muscovite + quartz + water. Eventually, sillimanite will form in micas, the site most favorable for nucleation, and begin to grow (point IV, Fig. 1a). When sillimanite grows from a mica, the reaction consumes aluminum and produces potassium, changing the conditions in the vicinity of the sillimanite. This will establish local equilibrium with the mineral assemblage muscovite + quartz + water + sillimanite. When this happens, the conditions near sillimanite will lie at the invariant point (K) on Fig. 2c, while the conditions near kyanite will lie at the invariant point (S) on Fig. 2c. The buffering of the activities of potassium and aluminum by local reactions creates chemical potential gradients between the kyanite and the sillimanite assemblages, resulting in the diffusion of aluminum from (S) to (K) and the diffusion of potassium in the opposite direction. The addition of aluminum and removal of potassium by transport through the matrix around the sillimanite results in the precipitation of sillimanite and dissolution of micas at the (K) invariant point. Similarly, the addition of potassium and removal of aluminum by transport through the matrix around kyanite causes kyanite to dissolve and micas to precipitate as the local mineral assemblage buffers the activities of aluminum and potassium at the (S) invariant point.

If the reaction and transport rates are high relative to the rate at which heat is being supplied to the rock, the local reactions will be able to consume heat at the same rate it enters the rock (FISHER, 1978) and keep the temperature close to the theoretical isograd (point III or IV, Fig. 1a). Under these conditions, nuclei will only form in a few of the most favorable sites, (YARDLEY, 1977; RIDLEY, 1985), local equilibrium will be maintained and a reaction mechanism will develop that uses material transport and mica catalysts to convert kyanite to sillimanite (Fig. 1c). If, on the other hand, the reactions are not able to buffer the temperature and it continues to rise (point V, Fig. 1a), sillimanite nuclei will form at many sites in the rock. Eventually, the reaction will be sufficiently overstepped to allow sillimanite to nucleate directly on kyanite (Fig. 1d). When this happens, local equilibrium will not be maintained because kyanite is in equilibrium with species having activities at (S) while the adjacent sillimanite will be in equilibrium with species having activities at (K) (Fig. 2c). The reaction will proceed by a non-equilibrium path, probably at conditions that lie in-between (K) and (S), until all

the kyanite in contact with sillimanite has been consumed. After kyanite is consumed, the conditions will migrate to (K) and local equilibrium will be re-established.

The factors controlling reaction mechanisms that take place in a rock when local equilibrium is maintained (*e.g.* Fig. 1c) can be examined in detail by constructing activity diagrams that show relationships among metastable phases in addition to those of the stable phases. An example of this type of diagram is shown in Fig. 3, which is the same activity diagram as Fig. 2c except that the metastable univariant lines and divariant fields are shown along with the stable ones. As in Fig. 2, the system is saturated with water at the *T* and *P* of interest and the standard states for the activities of potassium and aluminum are potassium oxide and corundum, respectively.

A total of twelve divariant fields are shown on Fig. 3. Each field represents a region in activity space where the mineral assemblages muscovite + water, quartz + water, sillimanite + water, and kyanite + water have a specific stability sequence. Following the notation convention of KUJAWA and EUGSTER (1966), the stability sequence of the four solid phases kyanite, sillimanite, muscovite, and quartz coexisting with water are shown by listing the first letters of the mineral names in a column in each of the twelve divariant fields. The letter representing the most stable mineral is at the bottom of the column and the letter representing the least stable mineral is at the top.

The twelve fields are separated by five univariant lines that represent equilibria among water and the mineral pairs muscovite + sillimanite [M + S], sillimanite + quartz [S + Q], muscovite + quartz [M + Q], kyanite + muscovite [K + M] and kyanite + quartz [K + Q]. When one of these lines is crossed, the stability sequence between the two minerals in equilibrium along the line reverses. For example, the fields separated by the line S + Q have quartz more stable than sillimanite on the side of the line where the aluminum activity is low and sillimanite more stable than quartz on the side of the line where aluminum activity is high. The segments of the univariant lines can be grouped into three types. Stable or first-order line segments are those which involve a switch in relative stability between the phases occupying the first and second stability levels in the divariant fields adjacent to the line. First-order line segments are shown as solid lines on Fig. 3. Second-order lines are those metastable segments of univariant lines that involve a switch in stability sequence between phases occupying the second and third stability levels in fields

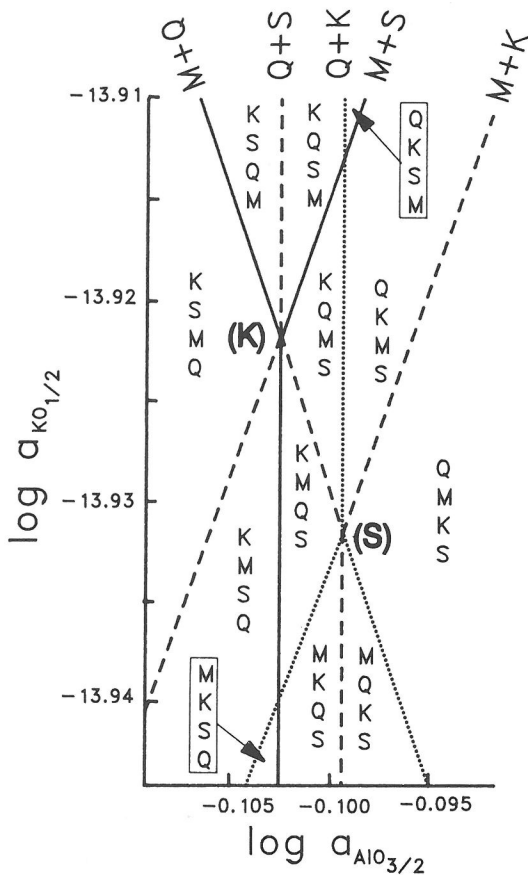


FIG. 3. Activity diagram at 627°C, 6 kb showing all stable and metastable invariant points, univariant lines and divariant fields involving the phases kyanite, sillimanite, muscovite and quartz. Water is present in all assemblages. K, S, M, and Q stand for kyanite, sillimanite, muscovite and quartz, respectively. The relative stability sequence of the phases in each divariant field is given by the columns of letters in each field. The mineral at the bottom of the list is the most stable, the one at the top is least stable. Each univariant line is labelled at the top of the diagram with the letters of the two minerals that are in equilibrium along it (e.g. M + Q). Stable (first-order) segments of univariant lines are shown as solid lines, second-order (metastable) segments of univariant lines are shown as dashed lines, and third-order (least stable) segments of univariant lines are shown as dotted lines. The kyanite-absent (K) invariant point is stable, the sillimanite-absent invariant point (S) is metastable.

adjacent to the line. Second-order line segments are shown as dashed lines on Fig. 3. Third-order lines are those that involve a switch in relative stability between phases occupying the third and fourth stability levels in divariant regions adjacent to the line. Third-order line segments are shown as dotted lines in Fig. 3.

Intersections of any two univariant lines involv-

ing a common phase produce invariant points representing three solid phases (plus water) in equilibrium. Invariant points always involve univariant line segments of two adjacent orders. There are two invariant points on Fig. 3: a stable one (K) formed by the intersection of first-order and second-order line segments and a metastable one (S) formed by the intersection of second-order and third-order line segments. Crossing of univariant lines that do not involve a common phase, such as M + K and S + Q, do not produce an invariant point because their energy levels differ by more than one order, so they do not intersect in free-energy space (KUNAWA and EUGSTER, 1966).

### GROWTH OF SILLIMANITE SEGREGATIONS

The constraints on material transport provided by local equilibrium with metastable mineral assemblages shown on Fig. 3 can be used to explain the reaction mechanisms that form sillimanite segregations in a rock containing kyanite porphyroblasts (Fig. 1c). At temperatures in the sillimanite stability field, prior to the nucleation of sillimanite (point III, Fig. 1a), the mineral assemblage kyanite + muscovite + quartz + water buffers the chemical potentials of aluminum and potassium, keeping conditions in the rock at the metastable sillimanite-absent invariant point (S). This invariant point slowly moves to higher activities of aluminum and potassium as temperature increases. Little reaction among the solid phases is required to maintain equilibrium because the fluid phase along the grain boundaries is not a large source or sink for components, due to its relatively small volume. When sillimanite nucleates in the rock (point IV, Fig. 1a), reactions take place that drive local conditions toward equilibrium with sillimanite. Although the amount of overstepping required for sillimanite nuclei to form is presently unknown, many workers (e.g. CHINNER, 1961) have made the observation that it is common for sillimanite at the lowest metamorphic grades to be only present in micas, suggesting micas have sites with activation energies that are most favorable for the formation of sillimanite nuclei. The reaction mechanisms and transport paths described below depend primarily on the types of minerals present at the site of nucleation rather than on the absolute amount of overstepping required to form the nuclei. Therefore, to facilitate discussion, an overstepping of 10°C was arbitrarily assumed to be required for sillimanite nuclei to form in muscovite.

Using this assumption, the first sillimanite to form in a rock containing kyanite + muscovite

+ quartz + water that is being metamorphosed along the isobaric path shown in Fig. 1a nucleates on muscovite at 627°C. The sillimanite-forming reaction will establish local equilibrium by driving the activities from those at (S) to those at (K). Due to the configuration of the metastable elements at 627°C and 6 kb (Fig. 3), changing from conditions at (S) to conditions at (K) must involve a decrease in the log of aluminum activity from a value of  $-0.0994$  to a value of  $-0.1026$  and an increase in the log of the potassium activity from a value of  $-13.931$  to a value of  $-13.922$ . The only reaction between sillimanite, muscovite, quartz and water that can produce these changes is a reaction that precipitates sillimanite and dissolves muscovite. The precise stoichiometry of the reaction depends upon the actual concentration changes of aluminum and potassium species in the grain boundary fluid that are required to produce the requisite changes in the activities of the components  $\text{AlO}_{3/2}$  and  $\text{KO}_{1/2}$ .

Once conditions corresponding to those at the invariant point (K) are established in the vicinity of sillimanite, the chemical potentials in the muscovite + quartz matrix surrounding sillimanite are forced by local equilibrium to lie along the metastable second-order portion of the univariant line M + Q that lies between (S) and (K) on Fig. 3. As long as cross-term diffusion coefficients (ANDERSON, 1981) are not important, this constraint on the chemical potentials in the matrix causes transport of aluminum toward the sillimanite and the transport of potassium away from it. The addition of aluminum and removal of potassium results in a reaction that forms sillimanite at the expense of muscovite.

This reaction keeps conditions at invariant point (K) by consuming the newly arrived aluminum and producing potassium to replace the amount that recently departed. The precise stoichiometry of this local reaction must be a linear combination of muscovite, sillimanite, quartz, and water plus the fluxes of material in and out of the volume of rock where the reaction takes place (FISHER, 1975). In the simplest case, where cross terms in the diffusion coefficient matrix are not important, the flux of a component  $i$  ( $J_i$ ) is related to the chemical potential gradient of the component  $i$  ( $d\mu_i/dx$ ) by a single thermodynamic diffusion coefficient ( $L_i$ ):

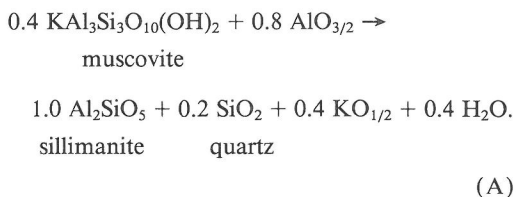
$$J_i = -L_i(d\mu_i/dx).$$

Because the ratio of chemical potential gradients transporting constituents between the invariant points (K) and (S) is fixed by the metastable second-order segment of the univariant line M + Q, the stoichiometry of the reaction at (S) is unique if the

ratio of the diffusion coefficients is specified (FISHER, 1975). For example, if the ratios of diffusion coefficients given by FOSTER (1981) are used, the ratio of the fluxes of aluminum and potassium in the M + Q matrix surrounding sillimanite are given by:

$$\begin{aligned} \frac{J_{\text{AlO}_{3/2}}}{J_{\text{KO}_{1/2}}} &= \frac{-L_{\text{AlO}_{3/2}} \text{grad } \mu_{\text{AlO}_{3/2}}}{-L_{\text{KO}_{1/2}} \text{grad } \mu_{\text{KO}_{1/2}}} \\ &= (6/1)(-1/3) = -2.0. \end{aligned} \quad (1)$$

Equation (1) means that two aluminum atoms are being supplied for every potassium atom removed from the region where sillimanite + muscovite + quartz is buffering the chemical potentials at (K). The only reaction between muscovite, quartz and sillimanite that can balance the material transport required by this flux ratio is:



This reaction, the overall reaction in the sillimanite segregation, consumes slightly more than 1.1 cc of muscovite and produces slightly less than 0.1 cc of quartz for every 1.0 cc of sillimanite produced.

Figure 4 shows how variation of the diffusion coefficient ratio of aluminum to potassium affects the stoichiometric coefficients for the overall reaction in the sillimanite segregation. The main effect of increasing the diffusion coefficient ratio of aluminum to potassium is to decrease the amount of

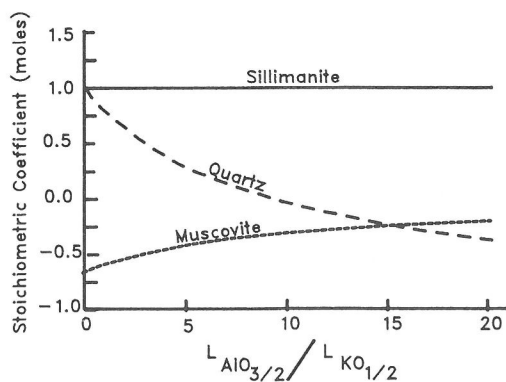


FIG. 4. The stoichiometry of the overall reaction within the sillimanite segregation as a function of the ratio of the aluminum and potassium diffusion coefficients. The stoichiometry given for this reaction in the text (reaction (A)) was calculated using  $(L_{\text{AlO}_{3/2}})/(L_{\text{KO}_{1/2}}) = 6$ .



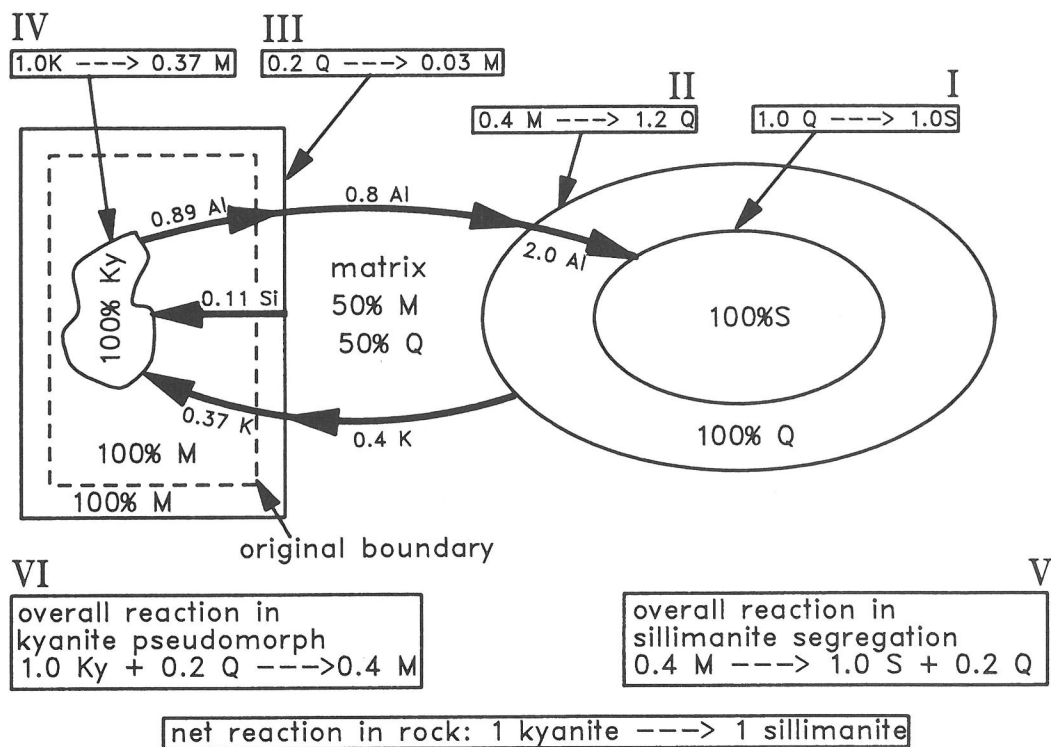


FIG. 5. Quantitative reaction model showing the sillimanite segregation and the kyanite pseudomorph produced when one mole of sillimanite grows at the expense of one mole of kyanite. The original boundary of the kyanite porphyroblast is given by a dashed line. Reaction interfaces in the segregation and pseudomorph are shown as thin lines and curves. The minerals involved in the reaction at each interface are given in the numbered boxes above the segregation and pseudomorph. These boxes, numbered I, II, III, and IV represent the local reactions (B), (C), (F) and (E), respectively. Material transport paths between reaction interfaces are shown by heavy lines with arrows giving the direction of transport for each component. Numbers and letters next to transport paths give moles of each component that diffused through each region of the rock when one mole of sillimanite is produced. Mineral modes for each part of the segregation and pseudomorph are given in volume %. The minerals involved in the overall reactions are given in boxes labelled V and VI, representing reactions (A) and (D), respectively. Ky, S, M, and Q stand for kyanite, sillimanite, muscovite and quartz, respectively. Al, Si and K stand for the transported components  $\text{AlO}_{3/2}$ ,  $\text{SiO}_2$  and  $\text{KO}_{1/2}$ , respectively. Diffusion coefficient ratios of  $(L_{\text{AlO}_{3/2}})/(L_{\text{KO}_{1/2}}) = 6$  and  $(L_{\text{SiO}_2})/(L_{\text{KO}_{1/2}}) = 5$  were used for the calculation of this diagram.

If the rock is closed to material transport beyond the hand-specimen scale, this reaction produces 1.1 cc of muscovite and consumes 0.9 cc of kyanite and 0.1 cc of quartz for every 1.0 cc of sillimanite that grows in the rock at another location. In this case, the amount of muscovite consumed by sillimanite growth exactly balances the amount of muscovite produced by kyanite dissolution. Similarly, the amount of quartz locally produced by sillimanite growth will be exactly balanced by the quartz consumed locally by kyanite dissolution. Thus, there is no net gain or loss of muscovite or quartz in the rock, they both serve as mineral catalysts which help the reaction kyanite  $\rightarrow$  sillimanite proceed.

The quartz required for reaction (D) is supplied either from quartz inclusions within the kyanite porphyroblast or from quartz in the matrix adjacent to the kyanite porphyroblast. If the kyanite porphyroblast contains more than 10% quartz inclusions, all of the quartz required for reaction (D) is available within the kyanite poikiloblast and reaction (D) will form a quartz + muscovite pseudomorph after the kyanite poikiloblast. The amount of quartz in the pseudomorph depends upon the volume percent of quartz inclusions in the kyanite poikiloblast that is replaced. For example, if the quartz inclusions make up 10% of the kyanite poikiloblast, then there will be 0.1 cc of quartz available locally for every 0.9 cc of kyanite that is consumed

by reaction (D). Since reaction (D) consumes 0.1 cc of quartz for every 0.9 cc of kyanite, the amount of quartz consumed by reaction (D) exactly equals the amount available and the pseudomorph that replaces kyanite is composed entirely of muscovite. However, if the modal amount of quartz in the poikiloblast is 25%, then there is 0.3 cc of quartz present locally for every 0.9 cc of kyanite. Reaction (D) consumes 0.1 cc of this quartz while consuming 0.9 cc of kyanite, leaving 0.2 cc of quartz mixed with the 1.1 cc of muscovite produced by reaction (D). A pseudomorph containing 15% quartz and 85% muscovite would result. In this circumstance, where there is quartz in the poikiloblast in excess of the amount required for reaction (D), the mineral assemblage within the pseudomorph and in the matrix is the same: muscovite + quartz. Coexisting muscovite and quartz cause the ratio of chemical potential gradients outside of the pseudomorph and within the pseudomorph to be identical because they both lie on the second order segment of the univariant line M + Q (Fig. 3). This constraint requires that no reaction takes place at the matrix/pseudomorph boundary. The original boundary of the kyanite poikiloblast is marked by the change in modes of muscovite and quartz between the amounts present in the matrix and the amounts produced in the pseudomorph by reaction (D). This boundary serves as an inert marker in the system, representing the bulk compositional difference between the matrix and the kyanite poikiloblast. In some instances, the matrix and pseudomorph modes will be nearly the same, making the pseudomorph difficult to recognize unless the pseudomorph micas are different in size or orientation from the matrix micas. Generally, the amount of muscovite in the pseudomorph is much higher than the amount in the matrix so the original boundary of the kyanite poikiloblast is easily recognized.

If there is no quartz in the kyanite porphyroblast, the silica for reaction (D) comes from the quartz in the matrix around the porphyroblast. In this circumstance, when kyanite first begins to dissolve, reaction (D) consumes quartz and kyanite at the porphyroblast boundary and replaces it with muscovite. A quartz-free muscovite rim will form between the dissolving kyanite and the matrix. The material transport to and from the kyanite/muscovite interface will be constrained by the Gibbs-Duhem relation of muscovite and the requirement that the reaction must be a linear combination of muscovite and kyanite. These constraints force the reaction to always produce muscovite when kyanite dissolves. The precise stoichiometry of the reaction depends upon the relative size of the diffusion coef-

ficients of silica, aluminum and potassium (Fig. 6). Values of  $L_{\text{AlO}_{3/2}}/L_{\text{KO}_{1/2}} = 6$  have been found to be compatible with a variety of textures in amphibolite facies pelites (FOSTER 1981, 1982, 1983, 1986). Figure 6 shows that if this value is used for  $L_{\text{AlO}_{3/2}}/L_{\text{KO}_{1/2}}$ , the reaction replacing kyanite with muscovite in the absence of quartz is relatively insensitive to the value of the diffusion coefficient of silica. For example, if  $L_{\text{AlO}_{3/2}}/L_{\text{KO}_{1/2}} = 6$ , the amount of muscovite produced per mole of kyanite consumed is 0.33 moles when  $L_{\text{SiO}_2}/L_{\text{KO}_{1/2}} = 0.001$  while it is 0.39 moles when  $L_{\text{SiO}_2}/L_{\text{KO}_{1/2}} = 50$ .

For a given set of diffusion coefficients, the reaction at the muscovite rim/matrix boundary can be calculated by subtracting the reaction at the kyanite/muscovite rim boundary from reaction (D), the net reaction for the entire pseudomorph. The exact stoichiometry of the reaction at the mica rim/matrix boundary depends upon the diffusion coefficient ratios. Figure 7 shows the effect that varying  $L_{\text{SiO}_2}/L_{\text{KO}_{1/2}}$  has on the stoichiometry of the reaction at the mica rim/matrix boundary of the kyanite pseudomorph. If the silica diffusion coefficient is low, the local reactions essentially conserve silica. If the silica diffusion coefficient is high, the local reactions produce silica at the mica rim/matrix boundary of the kyanite pseudomorph and transport the silica to a major sink at the kyanite/mica rim boundary in the interior of the pseudomorph. The texture produced in either case is very similar:

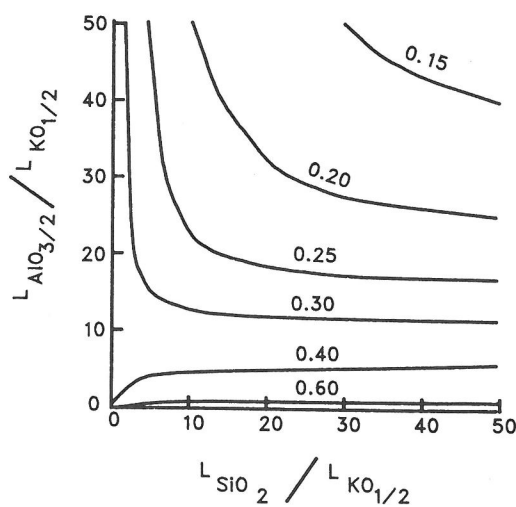


FIG. 6. Contours showing the moles of muscovite produced per mole of kyanite dissolved at the inner boundary of the quartz-free mica rim in the kyanite pseudomorph as a function of the ratio of the aluminum, potassium and silica diffusion coefficients. The stoichiometry of this reaction given in the text (reaction (E)) was calculated using  $(L_{\text{AlO}_{3/2}})/(L_{\text{KO}_{1/2}}) = 6$  and  $(L_{\text{SiO}_2})/(L_{\text{KO}_{1/2}}) = 5$ .

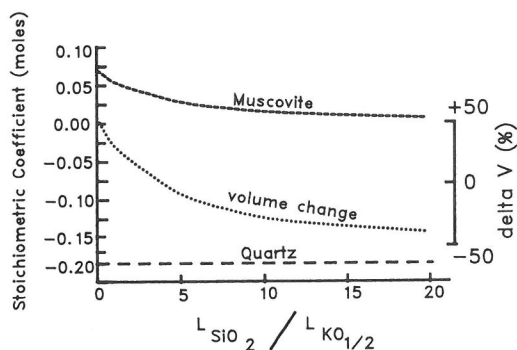
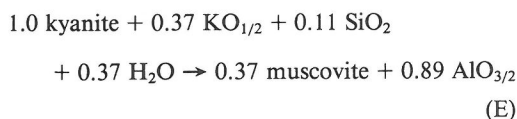


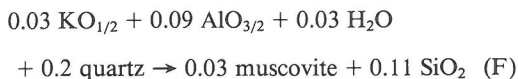
FIG. 7. The stoichiometry and volume change of the reaction at the mica rim/matrix boundary of the quartz-free mica pseudomorph after kyanite as a function of the ratio of the silica and potassium diffusion coefficients. The diffusion coefficient ratio of aluminum to potassium was held constant at a value of 6 to construct this diagram. The stoichiometry of this reaction given in the text (reaction (F)) was calculated using  $(L_{\text{AlO}_{3/2}})/(L_{\text{KO}_{1/2}}) = 6$  and  $(L_{\text{SiO}_2})/(L_{\text{KO}_{1/2}}) = 5$ .

kyanite is replaced by muscovite and a small amount of quartz in the matrix is converted to muscovite, forming a mica rim between the kyanite and matrix. The position of the original boundary between the kyanite and matrix is within the mica rim. The exact location of the original boundary depends upon the amount of quartz in the matrix and the stoichiometry of the reaction at the mica rim/matrix boundary.

The diffusion coefficient ratios also affect the delta V of reaction at the mica rim/matrix boundary. Low values of the silica diffusion coefficient result in reactions that produce substantially more muscovite than the amount of quartz that dissolves, resulting in a volume increase when matrix is converted to muscovite rim. High values of the silica diffusion coefficient result in reactions that produce almost no muscovite while dissolving substantial amounts of quartz, causing a volume loss when matrix is converted to muscovite rim. As shown in Fig. 7, a value of 5 for  $L_{\text{SiO}_2}/L_{\text{KO}_{1/2}}$  produces a matrix/pseudomorph reaction that essentially conserves volume. Using a value of 6 for the aluminum to potassium diffusion coefficient ratio and a value of 5 for the silica to potassium diffusion coefficient ratio gives:



for the reaction at the kyanite/mica rim interface and:



for the reaction at the mica rim/matrix boundary. The  $\text{SiO}_2$  in reactions (E) and (F) is the silica that is transported through the mica rim by diffusion. This silica is liberated by reaction (F) and consumed by reaction (E).

Reaction (F) consumes 0.1 cc of quartz and produces 0.1 cc of muscovite for every 1.0 cc of kyanite replaced by reaction (E). In a rock containing equal parts of muscovite and quartz, 0.2 cc of matrix will be required to supply the quartz for reaction (F). After the matrix has been converted to muscovite rim by reaction (F) it will contain 0.2 cc of muscovite, half of which was made by reaction (F). The other half is the 0.1 cc of muscovite originally in the matrix. If the muscovite produced by reaction (F) had a different grain size or orientation than the matrix muscovite, one would be able to identify the two different types. If the early and late muscovite were similar in size and orientation, then the old and new muscovites could not be distinguished in the mica rim that replaced matrix. The pseudomorph morphology, local reactions and material transport produced by reactions (E) and (F) are shown on the left side of Fig. 5.

#### CHEMICAL POTENTIAL PROFILES

The chemical potential gradients that drive material transport around the growing sillimanite and dissolving kyanite are primarily governed by the Gibbs-Duhem constraints provided by the matrix mineral assemblage muscovite + quartz + water. In the example shown in Fig. 5, the local reactions producing sillimanite and consuming kyanite form a muscovite-free zone around the sillimanite and a quartz-free zone around the kyanite. The removal of a matrix phase allows the chemical potentials to leave the M + Q metastable line between the (K) and (S) invariant points and pass through divariant fields, as shown in Fig. 8.

The chemical potentials within the muscovite-free mantle around the sillimanite pass through the divariant field where quartz is the second-most stable phase. The inner boundary (point I, Fig. 8) of the muscovite-free mantle is constrained to lie on the sillimanite + quartz line while the outer boundary of the muscovite-free mantle (point II, Fig. 8) is constrained to lie on the muscovite + quartz line. The chemical potential gradient of potassium within the muscovite-free mantle is zero because no potassium-bearing phases are present within the sillimanite segregation. The chemical potential gra-

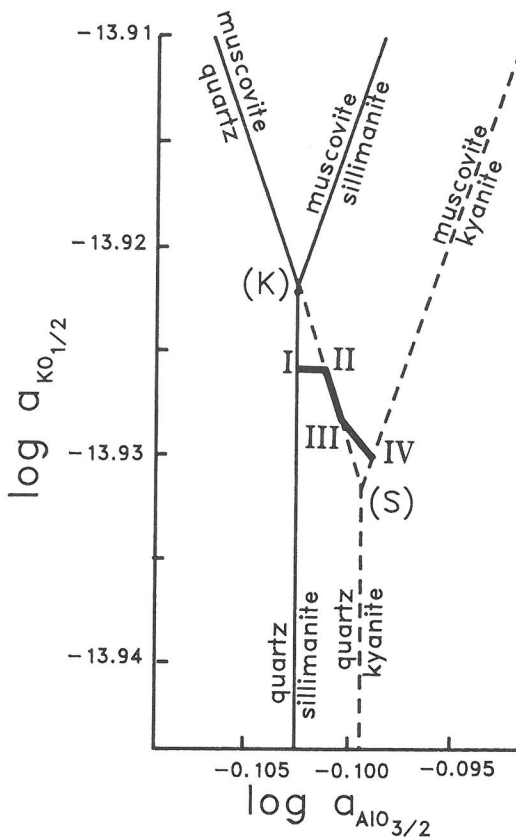


FIG. 8. Activity diagram showing conditions in the model illustrated in Fig. 5. Only selected portions of stable univariant lines (solid) and second-order univariant lines (dashed) are shown. Refer to Fig. 3 for complete diagram. Points I, II, III and IV correspond to reaction interfaces with the same numbers given in Fig. 5. The kyanite-absent and sillimanite-absent invariant points are labelled (K) and (S), respectively.

dient of aluminum within the muscovite-free mantle is governed by the width of the mantle and the difference in activities represented by the length of the line between points I and II on Fig. 8. As the sillimanite segregation grows and the width of the muscovite-free mantle increases, points I and II on Fig. 8 will gradually slide down the S + Q and M + Q univariant lines. This increases the chemical potential differences across the muscovite-free mantle so that the chemical potential gradients remain properly balanced with the gradients in the matrix to supply the constituents needed for reactions (B) and (C).

The chemical potentials within the quartz-free mica rim of the kyanite pseudomorph are represented by a line passing through the divariant field where muscovite is the second-most stable phase. Chemical potentials at the inner boundary of the

mica rim (point IV, Fig. 8) are constrained by the muscovite + kyanite assemblage, and the outer boundary (point III, Fig. 8) is constrained by the muscovite + quartz assemblage. The slope of the chemical potential profile between points III and IV is determined by the diffusion coefficient ratios and will not change as the pseudomorph grows. The magnitudes of the chemical potential gradients in the mica rim are determined by the width of the mica rim and the difference in chemical potentials corresponding to the length of the line between points III and IV. As the pseudomorph grows and the width of the mica rim increases, points III and IV will slide up the M + Q and M + K univariant lines to keep the chemical potential gradients in the mica rim balanced with the gradients in the matrix to supply the components needed for reactions (E) and (F). Eventually, when the last of the kyanite has been consumed, the chemical potentials in all domains of the rock will migrate back to values represented by invariant point (K) and reactions will cease.

## CONCLUSIONS

Most metamorphic reactions involve material transport on a local scale because the product minerals are only rarely the same composition as the substrate they grow on. The reaction mechanisms and transport paths that allow the overall reaction to proceed are usually strongly influenced by the constraints on material transport provided by mineral assemblages that are metastable with respect to the growing minerals. Construction of activity diagrams that include the geometric elements involving the metastable mineral assemblages can provide useful insight into the reaction mechanisms and the processes which control them. This approach can be coupled with the irreversible thermodynamic method devised by FISHER (1975, 1977) to develop quantitative models of reaction mechanisms that can be tested against textures observed in natural samples. Eventually, it should be possible to use these techniques to extract detailed pressure-temperature-time histories from textural features in metamorphic rocks.

*Acknowledgements*—I am indebted to Hans Eugster for teaching me about metastable elements of phase diagrams. Perceptive reviews by Bill Briggs, I-Ming Chou, George Fisher and Rick Sanford improved early versions of this manuscript. Calculations for this work were performed using computer equipment purchased with funds provided by a grant from the Amoco Foundation.

## REFERENCES

- ANDERSON D. E. (1981) Diffusion in electrolyte mixtures. In *Kinetics of Geochemical Processes* (eds. A. C. LASAGA

- and R. J. KIRKPATRICK), *Reviews in Mineral.* 8, Ch. 6, pp. 211–260. Mineral. Soc. Amer.
- BRADY J. B. (1975) Reference frames and diffusion coefficients. *Amer. J. Sci.* 275, 945–983.
- CARMICHAEL D. M. (1969) On the mechanism of prograde reactions in quartz-bearing pelitic rocks. *Contrib. Mineral. Petrol.* 20, 244–267.
- CARMICHAEL D. M. (1987) Induced stress and secondary mass transfer: thermodynamic basis for the tendency toward constant-volume constraint in diffusion metasomatism. In *Chemical Transport in Metasomatic Processes* (ed. H. C. HELGESON), pp. 239–264. Reidel.
- CHINNER G. A. (1961) The origin of sillimanite in Glen Cova, Angus. *J. Petrol.* 2, 312–323.
- EUGSTER H. P. and BAUMGARTNER L. (1987) Mineral solubilities and speciation in supercritical metamorphic fluids. In *Thermodynamic Modeling of Geological Materials: Minerals, Fluids, and Melts* (eds. I. S. E. CARMICHAEL and H. P. EUGSTER), *Reviews in Mineral.* 17, Ch. 10, pp. 367–404. Mineral. Soc. Amer.
- FISHER G. W. (1975) The thermodynamics of diffusion-controlled metamorphic processes. In *Mass Transport Phenomena in Ceramics* (eds. A. R. COOPER and A. H. HEUER), pp. 111–122. Plenum.
- FISHER G. W. (1977) Nonequilibrium thermodynamics in metamorphism. In *Thermodynamics in Geology* (ed. D. G. FRASER), pp. 381–403. Reidel.
- FISHER G. W. (1978) Rate laws in metamorphism. *Geochim. Cosmochim. Acta* 42, 1035–1050.
- FOSTER C. T. (1981) A thermodynamic model of mineral segregations in the lower sillimanite zone near Rangeley, Maine. *Amer. Mineral.* 66, 260–277.
- FOSTER C. T. (1982) Textural variation of sillimanite segregations. *Can. Mineral.* 20, 379–392.
- FOSTER C. T. (1983) Thermodynamic models of biotite pseudomorphs after staurolite. *Amer. Mineral.* 68, 389–397.
- FOSTER C. T. (1986) Thermodynamic models of reactions involving garnet in a sillimanite/staurolite schist. *Mineral. Mag.* 50, 427–439.
- HELGESON H. C., DELANY J. M., NESBITT H. W. and BIRD D. K. (1978) Summary and critique of the thermodynamic properties of rock-forming minerals. *Amer. J. Sci.* 278A, 1–229.
- KUJAWA F. B. and EUGSTER H. P. (1966) Stability sequences and stability levels in unary systems. *Amer. J. Sci.* 264, 620–642.
- RIDLEY J. (1985) The effect of reaction enthalpy on the progress of a metamorphic reaction. In *Metamorphic Reactions: Kinetics, Textures and Deformation* (eds. A. B. THOMPSON and D. C. RUBIE), pp. 80–97. Springer-Verlag.
- RIDLEY J. and THOMPSON A. B. (1986) The role of mineral kinetics in the development of metamorphic microtextures. In *Fluid-Rock Interactions during Metamorphism* (eds. J. V. WALTHER and B. J. WOOD), pp. 154–193. Springer-Verlag.
- WALTHER J. V. (1986) Mineral solubilities in supercritical H<sub>2</sub>O solutions. *Pure and Appl. Chem.* 58, 1585–1598.
- WOODLAND A. B. and WALTHER J. V. (1987) Experimental determination of the solubility of the assemblage paragonite, albite, and quartz in supercritical H<sub>2</sub>O. *Geochim. Cosmochim. Acta* 51, 365–372.
- YARDLEY B. W. D. (1977) The nature and significance of the mechanism of sillimanite growth in the Connemara Schists, Ireland. *Contrib. Mineral. Petrol.* 65, 53–58.
- YARDLEY B. W. D. (1989) *An Introduction to Metamorphic Petrology*. 248 pp. Longman.
- ZEN E-AN (1966) Construction of pressure-temperature diagrams for multi-component systems after the method of Schreinemakers—a geometric approach. *U.S. Geol. Surv. Bull.* 1125.